

Reactivity of cellulose during hydrothermal carbonization of lignocellulosic biomass

Maurizio Volpe^{a,b,*}, Antonio Messineo^a, Mikko Mäkelä^{c,d}, Meredith R. Barr^e, Roberto Volpe^e, Chiara Corrado^f, Luca Fiori^b

^a*Facoltà di Ingegneria e Architettura, Università degli Studi di Enna "Kore", Cittadella Universitaria, 94100, Enna, Italy*

^b*Dipartimento di Ingegneria Civile Ambientale e Meccanica, Università degli Studi di Trento, via Mesiano 77, 38123, Trento, Italy*

^c*Aalto University, School of Chemical Engineering, Department of Bioproducts and Biosystems, PO Box 16300, 00076 Aalto, Finland*

^d*Swedish University of Agricultural Sciences, Department of Forest Biomaterials and Technology, Skogsmarksgränd, 90183 Umeå, Sweden*

^e*Queen Mary University of London, Mile End Road, London E1 4NS, UK*

^f*University of Palermo, Department of BioMedicine, Neurosciences and Advanced Diagnostics (Bi.N.D), via Divisi 83, 90133 Palermo, Italy.*

*corresponding author: maurizio.volpe@unikore.it

Abstract

Hydrothermal carbonization of pure cellulose and birchwood samples was carried out at temperatures between 160 and 280 °C, 0.5 h residence time and biomass-to-water ratio of 20 wt% dry basis, to investigate HTC reactivity of cellulose naturally occurring lignocellulosic biomass. Pure cellulose samples remained unaltered at temperatures up to 220 °C, but significantly decomposed at 230 °C producing a thermal recalcitrant aromatic, high energy-dense material, showing lignin-like behavior. Fourier Transform Infrared spectroscopy (FTIR) showed dehydration and aromatization reactions occurring at temperatures equal or higher than 230 °C for pure cellulose samples while similar increase in aromatization for birchwood hydrochars was evident only at

(TGA) and FTIR suggest that a higher thermal resistance of natural occurring cellulose in birchwood (when compared to pure cellulose sample) could be related to a ‘protecting shield’ offered by interlinked lignin in the plant matrix.

31 **Keywords:** hydrothermal carbonization, solid biofuel, cellulose reactivity, birchwood,
32 acid hydrolysis

33 **Highlights:**

34 HTC induces decomposition of pure cellulose at temperature higher than 220 °C

35 HTC promotes aromatization of cellulose at temperature equal or higher than 230 °C

36 Cellulose decomposition in biomass is mitigated by lignin component during HTC

37 **1. Introduction**

38 The unrestrainable growth of global energy demand together with the increasing
39 environmental concern of using fossil fuel sources for energy production has prompted
40 government authorities to issue new regulations and renewable energy share targets.
41 EU-wide targets and policy objectives planned for 2030, within the 2030 climate and
42 energy framework, include: at least 40% cuts in greenhouse gas emissions (from 1990
43 levels), 32% share for renewable energy and 32.5% improvement in energy efficiency
44 [1]. To reach the EU 2030 targets and, in particular, the renewable energy ones, in the
45 last years the scientific community has boosted the study for the development of new
46 technologies for the production of thermal and electrical energy using alternative
47 renewable sources. Between the different renewable energy sources, biomass and, in
48 particular, residual organic materials offer several advantages. Residual biomass is
49 widely available in large amount at low cost, its conversion into an energy dense bio-
50 fuel and/or valuable carbon material represents an opportunity to decrease the amount of
51 waste with beneficial impact for the environment and human health [2]. Waste biomass
52 exploitation could be highly economically profitable for waste management companies
53 and represents a carbon-neutral and programmable energy source [3]. The conversion of

54 residual biomass into energy or valuable carbon-rich feedstock is affected by its high
55 moisture content, its perishability and low energy density. Anaerobic digestion (AD) of
56 wet residual biomass to produce methane-rich biogas represents one of the possible and
57 eco-sustainable route for increasing the renewable energy production while decreasing
58 green-house gas emissions [4]. However, the need for high initial investment costs and
59 the requirement for strict operating conditions has limited the widespread of AD, while
60 most of the operating plants are nowadays surviving owing mainly to economic
61 incentives [5]. Thermochemical technologies applied to conversion of residual
62 biomass such as torrefaction [6–8], slow and fast pyrolysis [9–11], gasification [12] or a
63 combination of these technologies [13] have been largely investigated in the last
64 decades but their widespread diffusion mainly failed due to the low energy efficiency,
65 especially for high moisture content biomass, and the low versatility due to the need of
66 very specific operating conditions strictly related to the nature, morphology and
67 physical and chemical composition of feedstock. In the more recent years, wet
68 thermochemical conversion of biomass is attracting more and more interest among
69 scientists and technology developers. Wet pyrolysis, also known as hydrothermal
70 carbonization (HTC), is carried out in water at sub-critical conditions, typically between
71 180 and 280 °C and at autogenous vapor pressure (10–60 bar). Water, at HTC reaction
72 conditions, promotes dehydration and decarboxylation of biomass, converting wet
73 residual organic material into a carbon-rich solid material, named hydrochar [14–16].
74 Comparative studies between dry thermochemical conversion and HTC of waste
75 biomass showed that the latter could be more energetically favorable, promoting higher
76 degree of carbonization of feedstock at same reaction temperatures [17]. Moreover,
77 hydrochars display significantly better energy and fuel qualities than the corresponding

78 pyrochars obtained at the same temperatures [18,19]. Since the rediscovery of wet
79 thermochemical treatment of biomass as a valuable process for CO₂ sequestration and
80 production of renewable solid biofuels [20–22], HTC has been used to convert many
81 kinds of waste biomass: lignocellulosic material as olive mill industry wastes [23]
82 loblolly pine [24]; agro-waste such as: tomato peel [25], orange waste [26], wheat straw
83 [27], food waste [28], organic fraction of municipal solid waste [29], paper mill industry
84 wastes [30–32], sewage sludge [33,34] and plastic wastes [35]. Despite the different
85 nature of the treated feedstock, most of the HTC works focused on the influence of the
86 operative variables like temperature, residence time and biomass to water ratio on the
87 energy, chemical and morphological properties of the produced hydrochars for their
88 possible applications as solid bio-fuels and valuable carbon materials (e.g. activated
89 carbons). According to our current knowledge, very few works attempted at describing
90 the evolution of biomass chemical structure during HTC [36], some studies reported the
91 reactivity of biomass macro-components during HTC albeit starting from commercially
92 available single components and none of them studied how biomass macro-constituents
93 reacted and/or interacted when intermeshed in lignocellulosic matrix [37–39].
94 Systematically larger char yields were observed from the pyrolysis of chemically
95 isolated lignin, compared to expected yields from the pyrolysis of lignin embedded in
96 plant material thus demonstrating that an entirely different reaction pathway is involved
97 when the constituents are embedded in plant material [40]. Nevertheless, unveiling the
98 evolution of reactivity of biomass macro-components during HTC is of great
99 importance to predict the properties of produced hydrochars. This work represents the
100 first study that uses TGA, FTIR and acid hydrolysis analysis, to prove that naturally
101 occurring lignin component interconnected in the biomass matrix could play a role in

102 increasing cellulose thermal resistance during HTC thus improving energy properties of
103 hydrochars.

104 **2. Materials and Methods**

105 *2.1 Material preparation and hydrothermal carbonization*

106 HTC of pure cellulose (Sigma Aldrich 50 μm) and dried birchwood, milled with a Retsch
107 SM2000 (Retsch GmbH) and sieved to grain size ≤ 1 mm, was carried out in an unstirred
108 50 ml batch reactor at 160, 180, 200, 220, 230, 240, 260 and 280 $^{\circ}\text{C}$, fixed 0.5 h residence
109 time and biomass-to-water ratio of 20 wt% on a dry basis. About 6.00 ± 0.05 g of dry
110 feedstock was loaded into the reactor and $30 \text{ g} \pm 0.5$ g of deionized water was added to it.
111 The mixture was carefully mixed, the reactor sealed, purged with pure nitrogen and heated
112 up to the set temperature (temperature increment of about 8-10 $^{\circ}\text{C}/\text{min}$) and left for the
113 set residence time. At the end of the reaction time the system was quenched by placing
114 the reactor on a large stainless steel disk kept at -30 $^{\circ}\text{C}$ and by blowing compressed air to
115 the reactor's walls. Once the system had reached a temperature of 30 $^{\circ}\text{C}$, the reactor's
116 outlet valve was opened and reaction gas collected in a graduated cylinder, previously
117 filled with water, to evaluate the produced gas volume. The gas mass yield was then
118 calculated assuming that gas was composed only of CO_2 . Hydrochar was then collected
119 by filtration and the solid residue dried in a conventional ventilated oven for at least 12
120 hours. Dried hydrochars were stored in sealed glass vials for further analysis and
121 characterization.

122 *2.2 Analytical determination and characterization*

123 The raw materials and hydrochars were subjected to acid hydrolysis to determine the
124 composition in macro-constituents. High Heating Value (HHV), elemental and proximate

125 composition in terms of Volatile Matter (VM), Fixed Carbon (FC) and Ash content and
126 attenuated Total Reflectance (ATR)_FTIR spectroscopy were also performed.

127 For acid hydrolysis the samples were first extracted with acetone according to the
128 guidelines of SCAN-CM 49:03. 250 mL acetone was used in a Soxhlet apparatus with 1
129 g of sample for 2 hours to guarantee removal of extractives and oils remaining on char
130 particles. The monosaccharide and lignin contents of the extractive-free samples were
131 then determined based on the National Renewable Energy Laboratory (NREL)
132 procedure for determination of structural components in biomass [41]. Sugar recovery
133 standards were prepared from analytical grade D-(+)-glucose, D-(+)-xylose, D-(+)-
134 galactose, D-(+)-mannose, L-(+)-arabinose and L-(+)-rhamnose. Hydrolysed monomers
135 were quantified after filtration based on respective peak areas using a Dionex ICS-3000
136 ion chromatograph (Dionex Corp.) and corrected to respective polymeric forms on a
137 dried, as-received basis [41]. Lignin contents were determined as the sum of
138 gravimetrically determined acid-insoluble lignin and acid-soluble lignin, which was
139 quantified with a Shimadzu UV-2550 spectrophotometer (Shimadzu Corp.) at 205 nm.
140 All acetone extractions and subsequent sugar and lignin determinations were performed
141 in duplicate with overall recoveries of 87-107% on a mass basis and a replicate root
142 mean squared error of 1.4% within a range of 0-99% glucan in the samples.

143 FTIR was carried out on a series of samples using a Perkin Elmer Spectrum 400 FT-
144 IR/NIR spectrometer (Perkin Elmer Inc., Tres Cantos, Madrid) in mid-IR mode,
145 equipped with a Universal ATR sampling device containing diamond/ZnSe crystal. The
146 spectra were recorded in the range from 650 to 4000 cm^{-1} , with a resolution of 4 cm^{-1} ,
147 by averaging 16 scans, spectra were baseline corrected and normalized.

148 The spectra were interpreted using a bilinear principal component analysis (PCA) model
149 based on absorbance units. The normalized transmittance IR spectra (Fig. S1) were first
150 converted into absorbance, further corrected for baseline offsets using the signals within
151 3600-4000 cm^{-1} and then mean centered for PCA (Fig. S2). The PCA results were given
152 through sample scores on the orthogonal principal components (PCs) and the respective
153 changes in the IR spectra illustrated through orthonormal PC loadings. The interested
154 reader is referred to the published literature on further details on the PCA method
155 [42,43].

156 Ultimate analyses were performed using a LECO 628 analyser equipped with Sulphur
157 module for CHN (ASTM D-5373 standard method) and S (ASTM D-1552 standard
158 method) content determination.

159 The HHV of solid samples was evaluated according to the CEN/TS 14918 standard by
160 means of an IKA C 200 calorimeter. Hydrochar mass yield (S_y) was calculated
161 according to Eq. (1):

$$162 \quad S_y = M_{HCdb}/M_{Rdb} \quad (1)$$

163 where M_{HCdb} represents the mass (dry basis) of the solid remaining after thermal
164 treatment (*i.e.* hydrochar), and M_{Rdb} represents the mass (dry basis) of the raw sample
165 before thermal treatment. Similarly, gas mass yield (G_y) was defined as the mass of gas
166 produced per unit mass of dry raw biomass sample. Liquid mass yield (L_y) was
167 calculated as the complement to 1 of the sum of S_y and G_y . The energy densification
168 ratio (EDR) was calculated according to Eq. (2), where HHV_{HCdb} represents the higher
169 heating value of hydrochar on a dry basis and HHV_{Rdb} represents the higher heating
170 value of the raw material. Energy yield (EY) was calculated according to Eq. (3).

171 $EDR = HHV_{HCdb}/HHV_{Rdb} \text{ (2)}$

172 $Ey = EDR * Sy \text{ (3)}$

173 Proximate analysis was carried out by means of TGA using a TA Instruments Q500
174 TGA. Between 2 and 20 mg of sample were placed in a 100 μ L platinum sample pan,
175 held at room temperature under high purity nitrogen at 60 mL/min (with an additional
176 40 mL/min balance protective gas) for 15 minutes, and then heated at 15 $^{\circ}$ C/min to 105
177 $^{\circ}$ C and held for 20 minutes at this temperature to remove moisture. Samples were
178 further heated at 15 $^{\circ}$ C/min to 900 $^{\circ}$ C and held for 7 minutes, and then cooled at 15
179 $^{\circ}$ C/min to 450 $^{\circ}$ C; the total mass loss from 105 $^{\circ}$ C through to this point as a portion of
180 the total sample mass on a dry ash-free basis is taken as VM. Samples were then heated
181 up at 15 $^{\circ}$ C/min to 750 $^{\circ}$ C in an equivalent flow of air, and held at this temperature for
182 15 min; the remaining mass as a portion of sample mass on a dry basis is taken as ash
183 content. FC on a dry ash-free basis was then calculated by subtracting Ash and VM
184 from the dry mass.

185 Sixteen different experiments (eight for cellulose and eight for birchwood) were carried
186 out at least in triplicate and average results are reported in tables and figures. cellulose
187 and birchwood hydrochars produced at different HTC temperature were coded CE_T
188 and BW_T respectively being “T” the value of process temperature expressed in
189 degrees Celsius.

190 **3. Results**

191 *3.1 Mass yields and hydrochar energy properties*

192 The summary of the results of cellulose and corresponding hydrochars in terms of mass
193 yields, energy properties (HHV, EY and EDR) and elemental, proximate analysis, H/C

and O/C atomic ratios are reported in tables 1 and 2 respectively. The data show on the one hand that cellulose did not appreciably degrade during HTC at temperatures lower than 220 °C, on the other hand, that at 230 °C cellulose underwent significant changes in mass yields and energy properties. When HTC temperature was increased from 220 to 230 °C, hydrochar mass yield dropped from 82.4 to 55.4 wt%, HHV increased from 17.2 MJ/kg to 21.8 MJ/kg, fixed carbon from 3.7 to 42.0 wt%, carbon content increased from 45.8 to 58.8 wt%. More evident changes in cellulose hydrochar composition occurred when temperature was raised to 240 °C, whereby HHV increased to 26.8 MJ/kg, however changes were reduced when further rising HTC temperature to 280 °C (HHV = 27.5 MJ/kg). The high changes in energy content and composition could be related to the breaking of the beta-glucosidic covalent bond that reportedly occurs at around 230 °C [36].

Table 1 – Cellulose HTC mass yields (wt%, d.b.), energy yields EY and EDR (%) d.b, HHV (MJ/kg) (Mass yields standard deviations < 1.5, HHV standard deviations < 0.05).

Sample	SY	GY	LY*	HHV _{HC}	EY	EDR
CE_raw	-	-	-	16.90	100.0	100.0
CE_160	98.3	0.1	1.6	17.03	99.0	100.8
CE_180	97.5	0.2	2.3	16.96	97.8	100.4
CE_200	95.5	0.2	4.2	16.95	95.8	100.3
CE_220	82.4	0.5	17.1	17.23	84.0	101.9
CE_230	55.4	2.0	42.6	21.76	71.4	128.8
CE_240	51.2	5.4	43.4	26.76	81.1	158.3
CE_260	50.9	7.8	41.3	27.03	81.4	159.9
CE_280	49.2	9.0	41.9	27.46	79.9	162.5

*Calculated by difference (LY=100-SY-GY)

As shown in table 2, VM, FC, ash content, carbon and hydrogen composition of cellulose hydrochars remained almost unaltered up to 220 °C. This corroborates the

mass yield and energy properties results. The sharp decrease of VM and corresponding increase of FC and C content at 230 °C confirm that a significant change in cellulose chemical composition occurred at that process temperature. Data also demonstrate that when further increasing HTC temperature, FC and C contents slightly increase while H content remains approximately constant or slowly decreases as commonly reported in HTC literature [25,29].

Table 2 – Cellulose raw and hydrochar proximate and elemental analyses. All values except from H/C and O/C atomic ratios in wt% d.b. (standard deviations for proximate and ultimate analysis < 1.2 and 0.2, respectively).

Sample	VM	FC	ASH	C	H	N	O*	H/C	O/C
CE_raw	97.7	2.4	0.0	45.1	5.5	0.0	49.4	1.44	0.82
CE_160	97.9	2.1	0.0	45.1	5.5	0.0	49.4	1.45	0.82
CE_180	97.8	2.2	0.0	45.2	5.5	0.0	49.3	1.45	0.82
CE_200	97.6	2.4	0.0	45.2	5.5	0.0	49.3	1.45	0.82
CE_220	96.3	3.7	0.0	45.8	5.5	0.0	48.7	1.42	0.80
CE_230	58.0	42.0	0.0	58.8	4.6	0.0	36.6	0.94	0.47
CE_240	58.0	42.0	0.0	70.5	3.9	0.1	25.5	0.67	0.27
CE_260	52.8	47.2	0.0	72.2	3.9	0.1	23.8	0.65	0.25
CE_280	52.6	47.4	0.3%	73.2	4.0	0.1	22.4	0.65	0.23

*Calculated by difference O = 100-Ash-C-H-N

HTC birchwood mass yields and energy properties results are shown in table 3 and proximate and elemental analysis are shown in table 4. Unlike pure cellulose hydrochars, birchwood hydrochars do not show sharp changes at any specific temperature. Mass yields, HHV, C and FC contents changed gradually with increasing reaction temperature. Significant body of evidence exists in the literature to demonstrate that, during hydrothermal reaction of lignocellulosic biomass, hemicellulose is more reactive than cellulose while lignin component is quite recalcitrant to degradation [37,44].

229 Table 3 – Birchwood HTC mass yields and energy properties (all values in wt% d.b.,
230 mass yields standard deviations < 0.9, HHV standard deviations < 0.3).

Sample	SY	GY	LY*	HHV _{HC}	EY	EDR
BW_raw	-	-	-	18.98	100.0	100.0
BW_160	92.0	0.3	7.7	18.73	90.8	98.7
BW_180	85.4	0.9	13.7	19.06	85.8	100.4
BW_200	70.9	1.6	27.5	20.18	75.4	106.3
BW_220	66.0	2.3	31.7	21.35	74.3	112.5
BW_230	62.3	3.6	34.2	22.69	74.4	119.5
BW_240	57.7	4.1	38.2	24.40	74.2	128.6
BW_260	53.3	7.4	39.3	27.05	75.9	142.5
BW_280	52.1	8.6	39.2	27.89	76.6	146.9

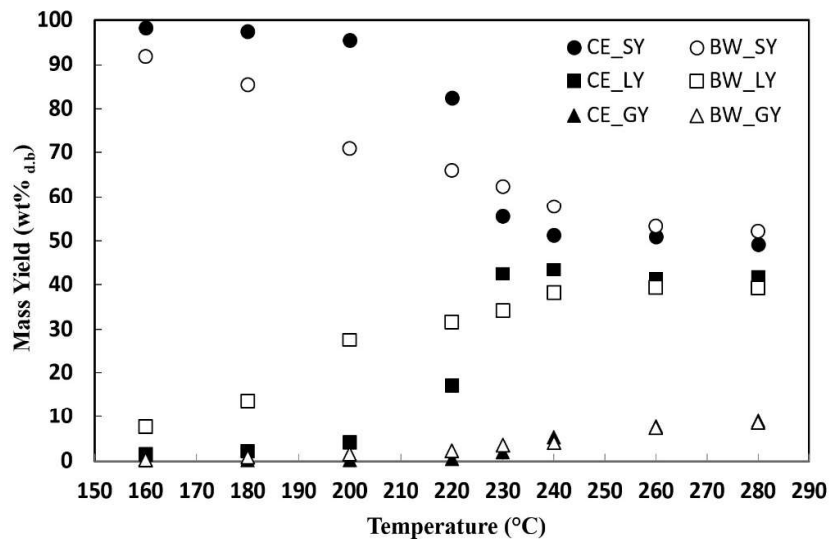
231 *Calculated by difference (LY=100-SY-GY)

232 Table 4 – Birchwood raw and hydrochar proximate and elemental analyses. All values
233 apart from H/C and O/C atomic ratios in wt% d.b. (standard deviations for proximate
234 and ultimate analysis < 1.6 and 0.2, respectively).

Sample	VM	FC	ASH	C	H	N	O*	H/C	O/C
BW_raw	87.8	12.2	0.3	50.4	5.4	0.1	43.8	1.28	0.65
BW_160	88.5	11.5	0.2	50.8	5.5	0.0	43.5	1.29	0.64
BW_180	86.5	13.5	0.2	51.9	5.5	0.1	42.3	1.25	0.61
BW_200	82.2	17.8	0.2	54.7	5.4	0.1	39.6	1.17	0.54
BW_220	77.4	22.6	0.2	57.7	5.2	0.1	37.0	1.08	0.48
BW_230	72.0	28.0	0.2	60.8	5.1	0.1	33.8	0.99	0.42
BW_240	62.4	37.6	0.2	66.5	4.8	0.2	28.4	0.86	0.32
BW_260	54.4	45.6	0.1	71.7	4.6	0.2	23.4	0.77	0.24
BW_280	50.8	49.2	0.1	73.2	4.6	0.2	21.8	0.75	0.22

235 *Calculated by difference O = 100-Ash-C-H-N

236 The initial decrease of HTC solid mass yield, faster than that observed for pure
237 cellulose, can be ascribed to the decomposition of extractives and hemicellulose
238 occurring at low HTC temperature (160-200 °C), figure 1.



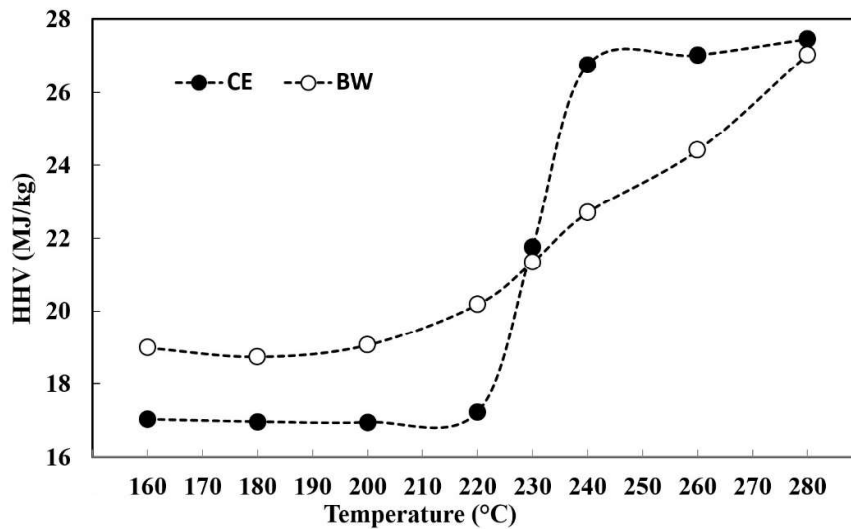
239

240 Fig. 1 Cellulose and birchwood HTC mass yields vs. HTC temperature (SY= solid
 241 yield, LY= liquid yield, GY= gas yield)

242 Figure 1 shows the comparison of mass yields changes of pure cellulose and birchwood
 243 hydrochars with HTC temperature. Notably, while cellulose solid yield remains
 244 approximately constant up to HTC temperature of 220 °C, birchwood hydrochar yield
 245 starts decreasing already at 160 °C, due to hydrolysis and/or removal of extractives first
 246 and hemicellulose degradation starting at about 180 °C [37]. The decrease of birchwood
 247 solid yield results in a liquid yield increase, while gas yields are negligible up to 230 °C
 248 and increase slowly up to approximately 9 wt% at 280 °C for both feedstock. After a
 249 sharp drop at 230 °C, cellulose hydrochar yields remained constant at approximately 50
 250 wt% between 240 and 280 °C, thereby demonstrating that no further significant
 251 degradation occurred at temperatures equal to or higher than 240 °C. Conversely,
 252 birchwood hydrochar samples showed mass yield progressively decreasing down to 52
 253 wt% at a HTC temperature of 280 °C. Mass yields results for both samples are
 254 consistent with the production and/or concentration of thermal resistant aromatic
 255 material under HTC condition [36,37]. Recent works demonstrated that HTC of residual

256 biomass occurring at higher temperatures can also improve the rate of back
257 polymerization of organics from the liquid to the solid phase, thus resulting in a
258 decrease of liquid yield and the production of secondary char [45,46].

259 Figure 2 shows trend in HHV changes vs. HTC temperature for cellulose when
260 compared to birchwood. cellulose hydrochar showed a 56% increase in HHV between
261 220 and 240 °C, while in the same range of HTC temperature HHV of the
262 corresponding birchwood hydrochars showed an increase of only 14%.



263
264 Fig. 2 Cellulose (CE) and birchwood (BW) HHV changes with HTC temperature

265 Van Krevelen plots for cellulose and birchwood samples reported in figure 3, show the
266 sharp differences in carbonization degree of cellulose hydrochars between the samples
267 produced at temperatures lower than 230 °C and those resulting from HTC performed
268 above 230 °C. Conversely, birchwood hydrochar samples show a progressive
269 carbonization with HTC temperature.

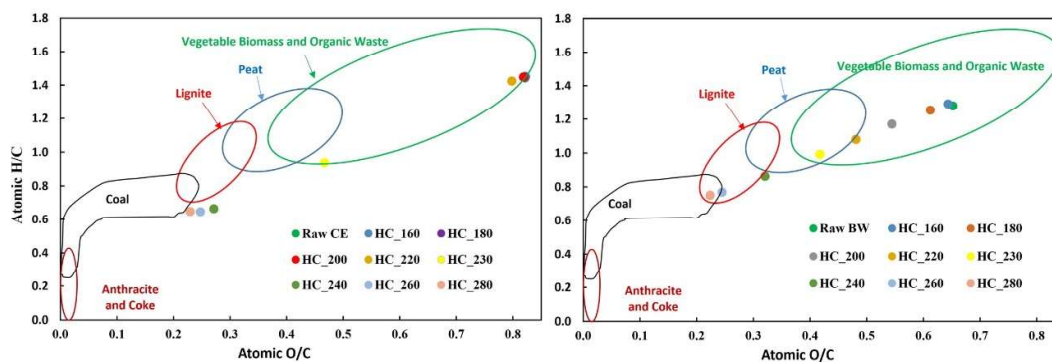


Fig. 3 Van Krevelen plots of Cellulose (left) and Birchwood (right) samples

3.2 Acid hydrolysis

Acid hydrolysis results, reported in table 5, show that the glucose fraction in pure cellulose sample, initially equal to approximately 99 wt%, decreased to 40 wt% at 230 °C and almost disappeared at 240 °C confirming the complete rupture of beta-glycosidic linkage of cellulose. The sharp decrease of the glucose fraction in cellulose hydrochar samples was accompanied by the increase of a lignin-like fraction with the production of more resistant aromatic structured compounds. Acid hydrolysis of birchwood show no evidence of such a sharp drop at 230 °C; conversely, the glucose fraction decreased more gradually with increasing HTC temperature confirming what recently reported in literature [44]. For example, at 240 °C cellulose and birchwood hydrochars showed a glucose fraction of 0.8 and 20.3 wt%, respectively, which suggests a sort of protective effect of the lignin content in the birchwood towards the cellulose content of the same feedstock .

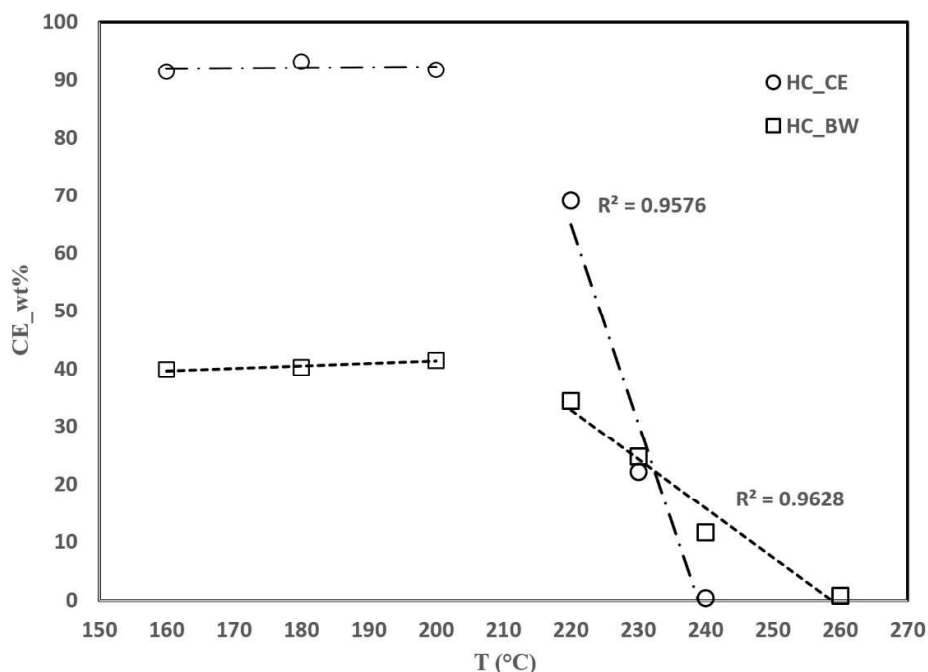
Table 5 – Acid hydrolysis analysis of raw cellulose and birchwood and corresponding hydrochars. All values in wt% d.b. Standard deviation of the data < 2.2.

Sample	Extractives	Lignin	Galactose	Glucose	Xylose	Mannose
CE_raw	0.0	0.0	b.d.l.	98.9	3.0	2.6
CE_160	0.0	0.0	b.d.l.	93.1	2.8	2.5

CE_180	0.0	0.0	b.d.l.	95.7	2.7	2.5
CE_200	0.0	0.0	b.d.l.	96.2	1.8	1.9
CE_220	3.0	9.0	b.d.l.	84.0	0.5	0.9
CE_230	24.0	40.0	b.d.l.	40.2	0.1	0.2
CE_240	21.0	74.0	b.d.l.	0.8	n.a.	n.a.
CE_260	21.0	79.0	b.d.l.	0.1	n.a.	n.a.
CE_280	16.0	79.0	b.d.l.	0.2	n.a.	n.a.
BW_raw	2.0	28.8	1.0	39.4	21.9	1.6
BW_160	4.0	20.5	0.6	43.4	18.3	1.5
BW_180	16.0	17.0	0.3	47.3	7.5	1.0
BW_200	26.0	15.0	0.1	58.7	2.0	0.3
BW_220	26.0	24.0	b.d.l.	52.4	0.2	0.1
BW_230	28.0	31.0	b.d.l.	39.9	0.1	0.1
BW_240	28.0	49.0	b.d.l.	20.3	0.1	0.0
BW_260	34.0	60.0	b.d.l.	1.6	0.1	n.a.
BW_280	34.0	61.0	b.d.l.	0.1	0.0	n.a.

287 b.d.l.: below detection limits

288 Figure 4 shows the change of cellulose percentage (normalized by the corresponding
289 hydrochar mass yield) vs. HTC temperature. Cellulose weight percentage in pure
290 cellulose and birchwood hydrochars shows a bi-modal trend depending on the HTC
291 reaction temperature. On the one hand, between 160 and 200 °C, cellulose in both series
292 of hydrochars is approximately constant; on the other hand, between 220 and 260 °C, it
293 decreased quickly, thereby showing linear trends. Notably, cellulose rate of
294 decomposition in birchwood was more than four times slower than pure cellulose
295 hydrochars. The lower rate of cellulose decomposition in birchwood could be associated
296 to the presence of interwoven lignin acting as a protecting shield in the lignocellulosic
297 matrix.



298

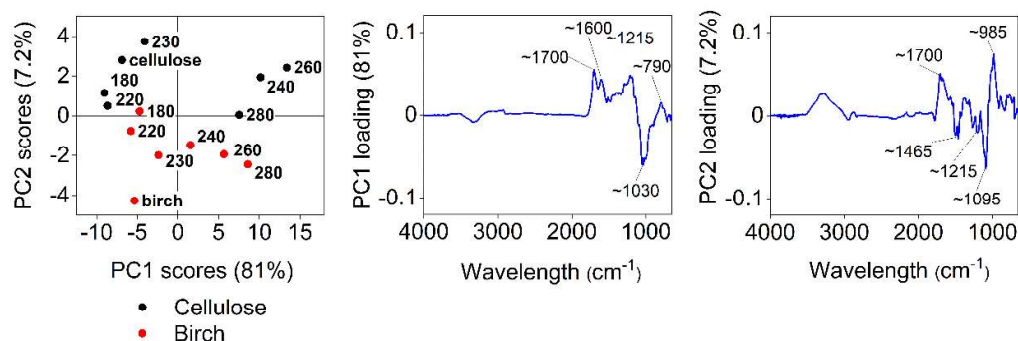
299 Fig. 4 Normalized cellulose weight component changes with HTC temperature in pure
300 cellulose and birchwood hydrochars

301 3.3 FTIR analysis

302 FTIR analysis has been widely used to investigate chemical and structural changes
303 occurring in biomass during HTC [36,47]. The PCA results based on the first two PCs
304 are illustrated in figure 5. In general, positive sample scores in PCA correspond to
305 increased absorbance on positive loadings. The same also applies with negative scores
306 and negative loadings. As illustrated in figure 5, the first PC explained 81% of the
307 variation in the absorbance spectra and mainly separated the samples based on HTC
308 temperature. Higher HTC temperatures hence lead to a decreased adsorbance at around
309 3300 cm⁻¹ attributable to dehydration reactions. Increased absorbance at around 2950-
310 3100 and 790 cm⁻¹ can be assigned to sp C-H stretching and bending out of plane modes
311 respectively, testifying a progressive aromatization of hydrochars with HTC
312 temperature. Moreover, the sharp increase of absorbance especially at approximately

1700 and 1215 cm^{-1} can be attributed to the free C=O stretching and bending modes due to cellulose beta-glucosidic linkage breaking [48]. The decrease in absorbance observed at around 1030 cm^{-1} provides evidence that pyranose structure of glucose is lost with increasing HTC temperature [49].

The second PC, which explained approximately 7% of the variation in the spectra, provided mainly a separation between the cellulose and birch wood samples. The cellulose samples showed consistently higher IR absorbance at 1700 and 985 cm^{-1} , probably due to higher concentration of free carbonyl (C=O) and aliphatic (C-O-C ether and alcohol C-O) respectively, due to pyranose structure breaking in cellulose hydrochar samples.

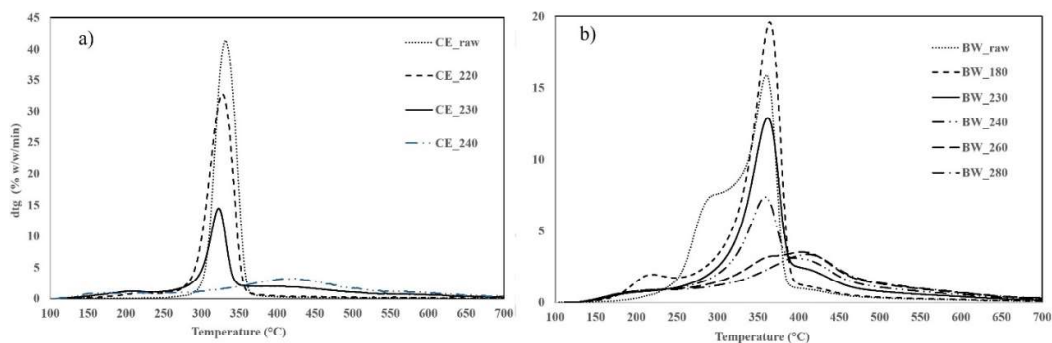


323

324 Fig. 5 Sample scores based on the first two PCs and the respective first (middle) and
325 second (right) PC loadings.

326 3.4 Derivative Thermogravimetric (DTG) analysis and cellulose reactivity

327 Figure 6a and b show DTG curves of cellulose and birchwood, respectively.



328

329 Fig. 6a, b DTG curves of: raw cellulose and selected cellulose hydrochars (a); raw
330 birchwood and selected birchwood hydrochars (b).

331 Graphs show a sharp decrease in reactivity of cellulose hydrochars above 230 °C and of
332 birchwood hydrochars above 240 °C. It may be noted that all birchwood samples are
333 significantly less reactive than cellulose samples as it is expected owing to the content
334 of lignin in birchwood (cellulose samples obviously do not contain any lignin). In
335 addition, reactivity decreases more sharply and faster with HTC temperature in cellulose
336 hydrochars when compared to birchwood hydrochar. However, the 240 °C birchwood
337 hydrochar sample shows some residual marginally higher reactivity than the pure
338 cellulose hydrochar. Again, probably this is related to the presence of lignin in
339 birchwood and the higher ‘resilience’ of the compounds formed during carbonisation.

340 4. Conclusions

341 This study sheds light on the role of lignin in cellulose decomposition in lignocellulosic
342 biomass. Cellulose component present in naturally occurring biomass matrix is less
343 reactive than free cellulose due to a ‘protecting shield’ offered by lignin. Mass yields,
344 energy properties, FTIR, DTG and acid hydrolysis analysis demonstrate that pure
345 cellulose is barely affected at a HTC temperature lower than 230 °C (residence time: 0.5
346 h) but severely degrades at a HTC temperature equal to or higher than 230 °C.

347 Conversely, natural occurring cellulose in birchwood degrades progressively at
348 increasing HTC temperature, decomposing completely at 280 °C.

349 **Declaration of competing interest**

350 The authors declared that they have no conflicts of interest to this work. We declare that
351 we do not have any commercial or associative interest that represents a conflict of
352 interest in connection with the work submitted.

353 **Acknowledgment**

354 We gratefully acknowledge the help of Paula Seppälä with the acid hydrolyses. This
355 research did not receive any specific grant from funding agencies in the public,
356 commercial, or not-for-profit sectors.

357

358 **References**

- 359 [1] European Commision, A policy framework for climate and energy in the period,
360 Communication From the Commission To the European Parliament, the Council,
361 the European Economic and Social Committee and the Committee of the
362 Regions. (2014) 18. [http://eur-lex.europa.eu/legal-](http://eur-lex.europa.eu/legal-content/EN/TXT/PDF/?uri=CELEX:52014DC0015&from=EN)
363 content/EN/TXT/PDF/?uri=CELEX:52014DC0015&from=EN.
- 364 [2] C. Gopu, L. Gao, M. Volpe, L. Fiori, J.L. Goldfarb, Valorizing municipal solid
365 waste: Waste to energy and activated carbons for water treatment via pyrolysis,
366 Journal of Analytical and Applied Pyrolysis. 133 (2018) 48–58.
367 <https://doi.org/10.1016/j.jaap.2018.05.002>.
- 368 [3] N.S. Bentsen, C. Felby, Biomass for energy in the European Union - A review of
369 bioenergy resource assessments, Biotechnology for Biofuels. 5 (2012) 1–10.
370 <https://doi.org/10.1186/1754-6834-5-25>.
- 371 [4] C. Mao, Y. Feng, X. Wang, G. Ren, Review on research achievements of biogas
372 from anaerobic digestion, Renewable and Sustainable Energy Reviews. 45 (2015)
373 540–555. <https://doi.org/10.1016/j.rser.2015.02.032>.
- 374 [5] L. Yang, F. Xu, X. Ge, Y. Li, Challenges and strategies for solid-state anaerobic
375 digestion of lignocellulosic biomass, Renewable and Sustainable Energy
376 Reviews. 44 (2015) 824–834. <https://doi.org/10.1016/j.rser.2015.01.002>.
- 377 [6] M.J. Prins, K.J. Ptasiński, F.J.J.G. Janssen, Torrefaction of wood Part 2. Analysis
378 of products, Journal of Analytical and Applied Pyrolysis. 77 (2006) 35–40.
379 <https://doi.org/10.1016/j.jaap.2006.01.001>.
- 380 [7] R. Volpe, A. Messineo, M. Millan, M. Volpe, R. Kandiyoti, Assessment of olive
381 wastes as energy source: pyrolysis, torrefaction and the key role of H loss in
382 thermal breakdown, Energy. 82 (2015) 119–127.
383 <https://doi.org/10.1016/j.energy.2015.01.011>.
- 384 [8] V. Benavente, A. Fullana, Torrefaction of olive mill waste, Biomass and
385 Bioenergy. 73 (2015) 186–194. <https://doi.org/10.1016/j.biombioe.2014.12.020>.
- 386 [9] Z. Li, N. Li, W. Yi, P. Fu, Y. Li, X. Bai, Design and operation of a down-tube
387 reactor demonstration plant for biomass fast pyrolysis, Fuel Processing
388 Technology. 161 (2017) 182–192. <https://doi.org/10.1016/j.fuproc.2016.12.014>.
- 389 [10] D. Chiaramonti, M. Prussi, M. Buffi, A.M. Rizzo, L. Pari, Review and
390 experimental study on pyrolysis and hydrothermal liquefaction of microalgae for
391 biofuel production, Applied Energy. 185 (2017) 963–972.
392 <https://doi.org/10.1016/j.apenergy.2015.12.001>.
- 393 [11] R. Volpe, J.M.B. Menendez, T.R. Reina, A. Messineo, M. Millan, Evolution of
394 chars during slow pyrolysis of citrus waste, Fuel Processing Technology. 158
395 (2017) 255–263. <https://doi.org/10.1016/j.fuproc.2017.01.015>.
- 396 [12] S. You, Y.S. Ok, S.S. Chen, D.C.W. Tsang, E.E. Kwon, J. Lee, C.H. Wang, A
397 critical review on sustainable biochar system through gasification: Energy and
398 environmental applications, Bioresource Technology. 246 (2017) 242–253.

399 <https://doi.org/10.1016/j.biortech.2017.06.177>.

400 [13] M.J. Prins, K.J. Ptasinski, F.J.J.G. Janssen, More efficient biomass gasification
401 via torrefaction, *Energy*. 31 (2006) 3458–3470.
402 <https://doi.org/10.1016/j.energy.2006.03.008>.

403 [14] A. Funke, F. Ziegler, Hydrothermal carbonization of biomass: A summary and
404 discussion of chemical mechanisms for process engineering, *Biofuels Bioproduct
405 & Biorefinery*. 4 (2010) 160–177. <https://doi.org/10.1002/bbb>.

406 [15] A. Kruse, A. Funke, M.-M. Titirici, Hydrothermal conversion of biomass to fuels
407 and energetic materials, *Current Opinion in Chemical Biology*. 17 (2013) 515–
408 521. <https://doi.org/10.1016/j.cbpa.2013.05.004>.

409 [16] S. Román, B. Ledesma, A. Álvarez, C. Coronella, S. V. Qaramaleki, Suitability
410 of hydrothermal carbonization to convert water hyacinth to added-value products,
411 *Renewable Energy*. 146 (2020) 1649–1658.
412 <https://doi.org/10.1016/j.renene.2019.07.157>.

413 [17] M. Volpe, L. Fiori, R. Volpe, A. Messineo, Upgrading of Olive Tree Trimmings
414 Residue as Biofuel by Hydrothermal Carbonization and Torrefaction: a
415 Comparative Study, *Chemical Engineering Transaction*. 50 (2016) 13–18.
416 <https://doi.org/10.3303/CET1650003>.

417 [18] Z. Liu, R. Balasubramanian, Upgrading of waste biomass by hydrothermal
418 carbonization (HTC) and low temperature pyrolysis (LTP): A comparative
419 evaluation, *Applied Energy*. 114 (2014) 857–864.
420 <https://doi.org/10.1016/j.apenergy.2013.06.027>.

421 [19] M. Pecchi, F. Patuzzi, V. Benedetti, R. Di Maggio, M. Baratieri,
422 Thermodynamics of hydrothermal carbonization: Assessment of the heat release
423 profile and process enthalpy change, *Fuel Processing Technology*. 197 (2020)
424 106206. <https://doi.org/10.1016/j.fuproc.2019.106206>.

425 [20] M.-M. Titirici, A. Thomas, M. Antonietti, Back in the black: hydrothermal
426 carbonization of plant material as an efficient chemical process to treat the CO₂
427 problem?, *New Journal of Chemistry*. 31 (2007) 787–789.
428 <https://doi.org/10.1039/b616045j>.

429 [21] A. Saba, P. Saha, M.T. Reza, Co-Hydrothermal Carbonization of coal-biomass
430 blend: Influence of temperature on solid fuel properties, *Fuel Processing
431 Technology*. 167 (2017) 711–720. <https://doi.org/10.1016/j.fuproc.2017.08.016>.

432 [22] N. Saha, A. Saba, M.T. Reza, Effect of hydrothermal carbonization temperature
433 on pH, dissociation constants, and acidic functional groups on hydrochar from
434 cellulose and wood, *Journal of Analytical and Applied Pyrolysis*. 137 (2019)
435 138–145. <https://doi.org/10.1016/j.jaap.2018.11.018>.

436 [23] M. Volpe, D. Wüst, F. Merzari, M. Lucian, G. Andreottola, A. Kruse, L. Fiori,
437 One stage olive mill waste streams valorisation via hydrothermal carbonisation,
438 *Waste Management*. 80 (2018) 224–234.
439 <https://doi.org/10.1016/j.wasman.2018.09.021>.

- 440 [24] M.T. Reza, M.H. Uddin, J.G. Lynam, S.K. Hoekman, C.J. Coronella,
441 Hydrothermal carbonization of loblolly pine: reaction chemistry and water
442 balance, *Biomass Conversion and Biorefinery*. 4 (2014) 311–321.
443 <https://doi.org/10.1007/s13399-014-0115-9>.
- 444 [25] E. Sabio, A. Álvarez-Murillo, S. Román, B. Ledesma, Conversion of tomato-peel
445 waste into solid fuel by hydrothermal carbonization: Influence of the processing
446 variables, *Waste Management*. 47 (2016) 122–132.
447 <https://doi.org/10.1016/j.wasman.2015.04.016>.
- 448 [26] E. Erdogan, B. Atila, J. Mumme, M.T. Reza, A. Toptas, M. Elibol, J. Yanik,
449 Characterization of products from hydrothermal carbonization of orange pomace
450 including anaerobic digestibility of process liquor, *Bioresource Technology*. 196
451 (2015) 35–42. <https://doi.org/doi.org/10.1016/j.biortech.2015.06.115>.
- 452 [27] M.T. Reza, E. Rottler, L. Herklotz, B. Wirth, Hydrothermal carbonization (HTC)
453 of wheat straw: Influence of feedwater pH prepared by acetic acid and potassium
454 hydroxide, *Bioresource Technology*. 182 (2015) 336–344.
455 <https://doi.org/10.1016/j.biortech.2015.02.024>.
- 456 [28] T. Wang, Y. Zhai, H. Li, Y. Zhu, S. Li, C. Peng, B. Wang, Z. Wang, Y. Xi, S.
457 Wang, C. Li, Co-hydrothermal carbonization of food waste-woody biomass
458 blend towards biofuel pellets production, *Bioresource Technology*. 267 (2018)
459 371–377. <https://doi.org/10.1016/j.biortech.2018.07.059>.
- 460 [29] M. Lucian, M. Volpe, L. Gao, G. Piro, J.L. Goldfarb, L. Fiori, Impact of
461 hydrothermal carbonization conditions on the formation of hydrochars and
462 secondary chars from the organic fraction of municipal solid waste, *Fuel*. 233
463 (2018) 257–268. <https://doi.org/doi.org/10.1016/j.fuel.2018.06.060>.
- 464 [30] M. Mäkelä, V. Benavente, A. Fullana, Hydrothermal carbonization of industrial
465 mixed sludge from a pulp and paper mill, *Bioresource Technology*. 200 (2016)
466 444–450. <https://doi.org/10.1016/j.biortech.2015.10.062>.
- 467 [31] H. Wikberg, T. Ohra-aho, M. Honkanen, H. Kanerva, A. Harlin, M. Vippola, C.
468 Laine, Hydrothermal carbonization of pulp mill streams, *Bioresource*
469 *Technology*. 212 (2016) 236–244. <https://doi.org/10.1016/j.biortech.2016.04.061>.
- 470 [32] Z. Al-Kaabi, R. Pradhan, N. Thevathasan, A. Gordon, Y.W. Chiang, A. Dutta,
471 Bio-carbon production by oxidation and hydrothermal carbonization of paper
472 recycling black liquor, *Journal of Cleaner Production*. 213 (2019) 332–341.
473 <https://doi.org/10.1016/j.jclepro.2018.12.175>.
- 474 [33] Y. Zhai, X. Liu, Y. Zhu, C. Peng, T. Wang, L. Zhu, C. Li, G. Zeng,
475 Hydrothermal carbonization of sewage sludge: The effect of feed-water pH on
476 fate and risk of heavy metals in hydrochars, *Bioresource Technology*. 218 (2016)
477 183–188. <https://doi.org/10.1016/j.biortech.2016.06.085>.
- 478 [34] F. Merzari, M. Langone, G. Andreottola, L. Fiori, Methane production from
479 process water of sewage sludge hydrothermal carbonization. A review.
480 Valorising sludge through hydrothermal carbonization, *Critical Reviews in*
481 *Environmental Science and Technology*. 49 (2019) 947–988.

482 <https://doi.org/10.1080/10643389.2018.1561104>.

483 [35] M.E. Iñiguez, J.A. Conesa, A. Fullana, Hydrothermal carbonization (HTC) of
 484 marine plastic debris, *Fuel*. 257 (2019) 116033.
 485 <https://doi.org/10.1016/j.fuel.2019.116033>.

486 [36] X. Zhuang, H. Zhan, Y. Song, C. He, Y. Huang, X. Yin, Insights into the
 487 evolution of chemical structures in lignocellulose and non lignocellulose
 488 biowastes during hydrothermal carbonization (HTC), *Fuel*. 236 (2019) 960–974.
 489 <https://doi.org/10.1016/j.fuel.2018.09.019>.

490 [37] A.M. Borrero-lópez, E. Masson, A. Celzard, V. Fierro, Modelling the reactions
 491 of cellulose, hemicellulose and lignin submitted to hydrothermal treatment,
 492 *Industrial Crops & Products*. 124 (2018) 919–930.
 493 <https://doi.org/10.1016/j.indcrop.2018.08.045>.

494 [38] X. Lu, P.J. Pellechia, J.R.V. Flora, N.D. Berge, Influence of reaction time and
 495 temperature on product formation and characteristics associated with the
 496 hydrothermal carbonization of cellulose, *Bioresource Technology*. 138 (2013)
 497 180–190. <https://doi.org/10.1016/j.biortech.2013.03.163>.

498 [39] Y. Gao, X.H. Wang, H.P. Yang, H.P. Chen, Characterization of products from
 499 hydrothermal treatments of cellulose, *Energy*. 42 (2012) 457–465.
 500 <https://doi.org/10.1016/j.energy.2012.03.023>.

501 [40] A. George, T.J. Morgan, R. Kandiyoti, Pyrolytic Reactions of Lignin within
 502 Naturally Occurring Plant Matrices: Challenges in Biomass Pyrolysis Modeling
 503 Due to Synergistic Effects, *Energy & Fuels*. 28 (2014) 6918–6927.
 504 <https://doi.org/10.1021/ef501459c>.

505 [41] a. Sluiter, B. Hames, R. Ruiz, C. Scarlata, J. Sluiter, D. Templeton, D. Crocker,
 506 NREL/TP-510-42618 analytical procedure - Determination of structural
 507 carbohydrates and lignin in Biomass, Laboratory Analytical Procedure (LAP).
 508 (2012) 17. <https://doi.org/NREL/TP-510-42618>.

509 [42] P. Geladi, Chemometrics in spectroscopy. Part 1. Classical chemometrics,
 510 *Spectrochimica Acta - Part B Atomic Spectroscopy*. 58 (2003) 767–782.
 511 [https://doi.org/10.1016/S0584-8547\(03\)00037-5](https://doi.org/10.1016/S0584-8547(03)00037-5).

512 [43] R. Bro, A.K. Smilde, Principal component analysis, *Analytical Methods*. 6
 513 (2014) 2812–2831. <https://doi.org/10.1039/c3ay41907j>.

514 [44] M. Mäkelä, M. Volpe, R. Volpe, L. Fiori, O. Dahl, Spatially resolved spectral
 515 determination of polysaccharides in hydrothermally carbonized biomass, *Green*
 516 *Chemistry*. 20 (2018) 1114–1120. <https://doi.org/10.1039/C7GC03676K>.

517 [45] M. Lucian, M. Volpe, L. Fiori, Hydrothermal Carbonization Kinetics of
 518 Lignocellulosic Agro-Wastes: Experimental Data and Modeling, *Energies*. 516
 519 (2019). <https://doi.org/10.3390/en12030516>.

520 [46] M. Volpe, L. Fiori, From olive waste to solid biofuel through hydrothermal
 521 carbonisation: The role of temperature and solid load on secondary char
 522 formation and hydrochar energy properties, *Journal of Analytical and Applied*

- 523 Pyrolysis. 124 (2017) 63–72. <https://doi.org/doi.org/10.1016/j.jaap.2017.02.022>.
- 524 [47] M.T. Reza, W. Becker, K. Sachsenheimer, J. Mumme, Hydrothermal
525 carbonization (HTC): Near infrared spectroscopy and partial least-squares
526 regression for determination of selective components in HTC solid and liquid
527 products derived from maize silage, *Bioresource Technology*. 161 (2014) 91–
528 101. <https://doi.org/doi.org/10.1016/j.biortech.2014.03.008>.
- 529 [48] W. Peng, L. Wang, M. Ohkoshi, M. Zhang, Separation of hemicelluloses from
530 Eucalyptus species: Investigating the residue after alkaline treatment, *Cellulose*
531 *Chemistry and Technology*. 49 (2015) 757–764.
- 532 [49] A. Álvarez-Murillo, E. Sabio, B. Ledesma, S. Rom, Generation of biofuel from
533 hydrothermal carbonization of cellulose. *Kinetics modelling, Energy*. 94 (2016)
534 600–608. <https://doi.org/10.1016/j.energy.2015.11.024>.
- 535

Declaration of interests

☐ The authors declare that they have no known competing financial interests or personal relationships that could have appeared to influence the work reported in this paper.

☐ The authors declare the following financial interests/personal relationships which may be considered as potential competing interests:

--

Supplementary Materials

Reactivity of cellulose during hydrothermal carbonization of lignocellulosic biomass

Maurizio Volpe^{a,b,*}, Antonio Messineo^a, Mikko Mäkelä^{c,d}, Meredith R. Barr^e, Chiara Corrado^f, Roberto Volpe^e, Luca Fiori^b

Fig. S1a, b report FTIR spectra of Cellulose (a) and Birchwood (b) of raw and hydrochars samples at different HTC temperatures.

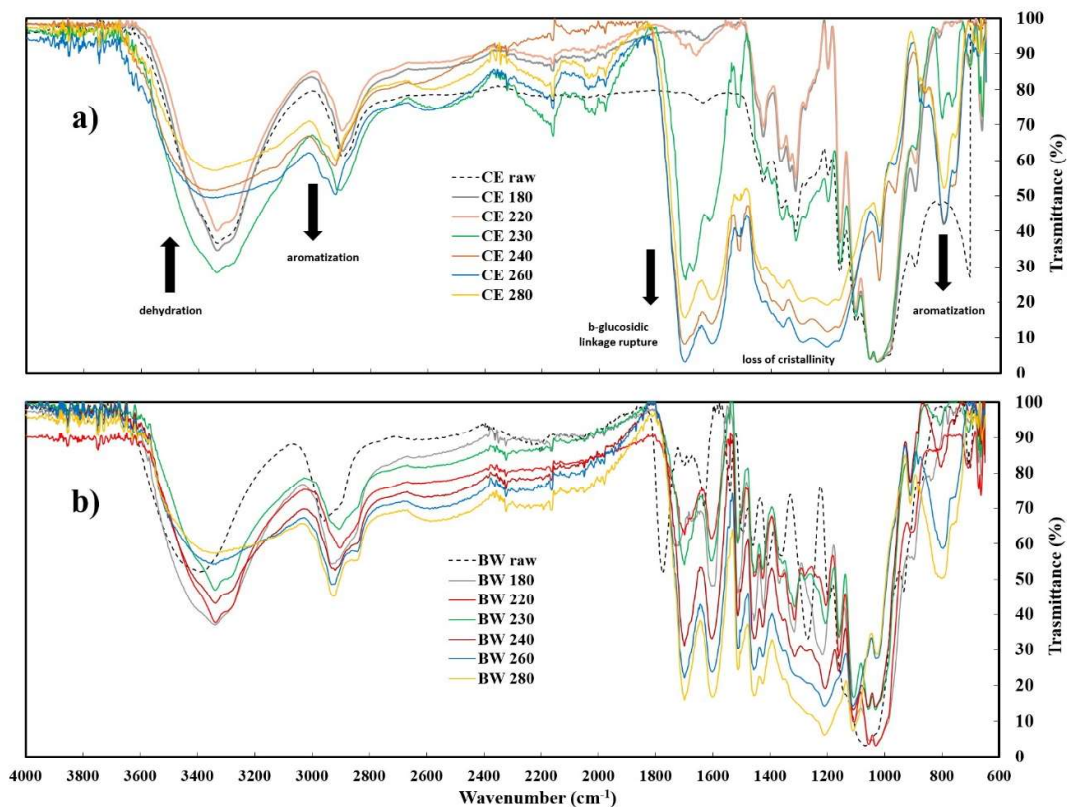


Fig. S1a, b FTIR spectra of Cellulose (a) and Birchwood (b) raw and corresponding hydrochars

Figure S2 reports the normalized FTIR spectra transmittance and their conversion into absorbance spectra for Principal Component Analysis, (PCA) of Cellulose and Birchwood raw and hydrochar samples at different HTC temperature.

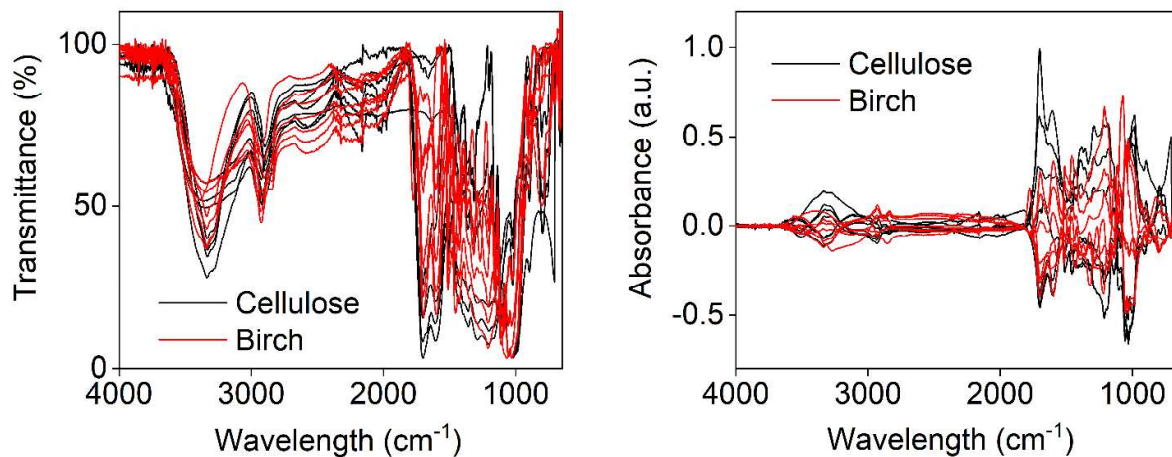


Fig. S2: The FTIR spectra after baseline correction and normalization in transmittance (% , left) and the preprocessed spectra in absorbance units before PCA (right).